"Eyes on the Street"
Estimating Natural Surveillance Along Amsterdam's City Streets Using Street-Level Imagery

van Asten, T.; Milias, V.; Bozzon, A.; Psyllidis, A.

DOI
10.1007/978-3-031-31746-0_12

Publication date
2023

Document Version
Final published version

Published in
Intelligence for Future Cities

Citation (APA)
van Asten, T., Milias, V., Bozzon, A., & Psyllidis, A. (2023). "Eyes on the Street": Estimating Natural Surveillance Along Amsterdam's City Streets Using Street-Level Imagery. In R. Goodspeed, R. Sengupta, M. Kyttä, & C. Pettit (Eds.), *Intelligence for Future Cities: Planning Through Big Data and Urban Analytics* (pp. 215-229). (The Urban Book Series). Springer. https://doi.org/10.1007/978-3-031-31746-0_12

Chapter 12
"Eyes on the Street": Estimating Natural Surveillance Along Amsterdam's City Streets Using Street-Level Imagery

Timo Van Asten, Vasileios Milias, Alessandro Bozzon, and Achilleas Psyllidis

Abstract Neighborhood safety and its perception are important determinants of citizens' health and well-being. Contemporary urban design guidelines often advocate urban forms that encourage natural surveillance or "eyes on the street" to promote community safety. However, assessing a neighborhood's level of natural surveillance is challenging due to its subjective nature and a lack of relevant data. We propose a method for measuring natural surveillance at scale by employing a combination of street-level imagery and computer vision techniques. We detect windows on building facades and calculate sightlines from the street level and surrounding buildings across forty neighborhoods in Amsterdam, the Netherlands. By correlating our measurements with the city's Safety Index, we also validate how our method can be used as an estimator of neighborhood safety. We show how perceived safety varies with window level and building distance from the street, and we find a non-linear relationship between natural surveillance and (perceived) safety.

Keywords Natural surveillance · Perceived safety · Crime · Eyes on the street · Street-level imagery

T. Van Asten
Dutch Ministry of the Interior and Kingdom Relations, The Hague, The Netherlands

V. Milias (✉) · A. Bozzon · A. Psyllidis
Faculty of Industrial Design Engineering, Delft University of Technology, Landbergstraat 15, 2628CE Delft, The Netherlands
e-mail: v.milias@tudelft.nl

A. Bozzon
e-mail: a.bozzon@tudelft.nl

A. Psyllidis
e-mail: a.psyllidis@tudelft.nl

R. Goodspeed et al. (eds.), *Intelligence for Future Cities*, The Urban Book Series,
https://doi.org/10.1007/978-3-031-31746-0_12

12.1 Introduction

Safe outdoor environments contribute substantially to a neighborhood's level of livability. A growing body of literature has shown that the design and structure of the built environment can influence both actual safety risks and how safety is perceived by different population groups, subsequently impacting citizens' physical and mental health and well-being (Foster and Giles-Corti 2008; Jackson and Stafford 2009; Mason et al. 2013; Stafford et al. 2007). Especially in neighborhoods where the fear of crime is disproportionate to the actual crime rates, there is evidence of significant associations with lower levels of physical activity (e.g., limited play among children and walking in older populations, or women being discouraged from using parts of the neighborhood), leading to increased levels of childhood obesity and social isolation amongst the elderly (Barnett et al. 2017; Groshong et al. 2020; Won et al. 2016).

Design and planning approaches to community safety in urban spaces, including Newman's defensible space theory (Newman 1972) and the Crime Prevention Through Environmental Design (CPTED) strategic framework (Crowe 2000), often advocate for neighborhoods with increased density, mixture of land uses, well-maintained walkways, and permeable street networks with high connectivity, even though there has been some recent criticism about the universality of these features in reducing actual crime risk and the fear of crime (Barton 2010; Cozens 2015; Cozens and Hillier 2012; Rydin et al. 2012). Similar principles are also adopted by the recent United Nations' guidelines on safer cities and human settlements (UN-Habitat 2020).

A common denominator across theories and design approaches aimed at improving actual and perceived safety is the provision of *natural* (or *passive*) *surveillance* in urban public spaces (Crowe 2000). Originating in what Jane Jacobs referred to as "eyes on the street" (Jacobs 1961), enhancing a neighborhood's level of natural surveillance has become a widely adopted design guideline towards safer urban environments (Carmona 2021; UN-Habitat 2020). Natural surveillance is a byproduct of how citizens normally and routinely use public spaces (Crowe 2000). Even though there are several factors that can influence the level of natural surveillance, it is generally assumed that characteristics such as good street lighting, abundance of unobstructed windows overlooking walkways, and more permeable streets contribute to an increased level of natural surveillance (Cozens 2015; Foster et al. 2011). However, evidence of how much of these built-environment characteristics contribute to increased natural surveillance and lead to improved perceptions of safety is still lacking. Several approaches to measuring natural surveillance have been proposed to date, ranging from collecting observations on the ground (Lee et al. 2017; Peeters and Vander Beken, 2017; Reynald and Elffers 2009) to computational models for estimating sightlines (Amiri and Crain 2020; Shach-Pinsly 2019). Yet, measurements across large spatial extents remain a challenge even for computational approaches, primarily due to the subjective nature of surveillance and the lack of relevant fine-grained data.

This paper addresses these knowledge gaps, first, by introducing a method for measuring natural surveillance at scale using street-level imagery and computer vision techniques and, second, by providing evidence of a non-linear relationship between natural surveillance and (perceived) safety. We collected and analyzed street- level imagery along all street segments across 40 neighborhoods in the city of Amsterdam, the Netherlands. Unlike related approaches that use generic proxies of visibility such as the distance between buildings (De Nadai et al. 2020; Shach-Pinsly 2019), street-level imagery gives us the opportunity to capture built-environment features that can affect natural surveillance, such as the location of windows on a building facade and any visibility blockages by fences or vegetation.

We extracted these features with geolocalization and computer vision (i.e., facade labeling) techniques. We calculated sightlines from the windows to each street and vice versa, as well as the windows of surrounding buildings, using the extracted features. Drawing on the work of (Peeters and Vander Beken 2017) and (Amiri and Crain 2020), we calculated two types of surveillance for each street segment: (1) *street surveillance*, which captures the surveillance of windows from the street level and vice versa, and (2) *occupant surveillance*, which captures the surveillance of windows from surrounding buildings. We then correlated the resulting surveillance values per street segment with publicly available data on (perceived) safety, crime, and nuisance in Amsterdam. Our research goes beyond defining the magnitude of associations between natural surveillance and (perceived) safety by identifying street-segment surveillance threshold values above which the feeling of safety remains unchanged. Such evidence can have significant implications for the design of safer neighborhoods and communities.

The remainder of this paper is structured as follows. We first present our research methods and describe the data sources, the study area, and how we calculated the sightlines and measure street and occupant surveillance. We then report the results of our analysis of Amsterdam's neighborhoods, and correlate them with the Amsterdam Safety Index. Next, we discuss the outcomes of our analysis, identify threshold values and implications for the design of safer communities. Finally, we summarize the conclusions and suggest future lines of research.

12.2 Method

We estimated natural surveillance at the street-segment level considering both *street* and *occupant* surveillance[1]. Both of these surveillance types depend on the degree to which people are able to observe the street from a specified distance; what is usually referred to as *sightline*. We grouped sightlines according to three parameters. The first parameter was based on the assumption that surveillance from ground floor windows is associated with lower levels of street crime than surveillance from up-

[1] The source code of our method is available on GitHub: https://github.com/timovanasten/natural-surveillance.

per floor windows, which is supported by previous research (Lee et al. 2017). We grouped sightlines based on their altitude $a_{\max}$ to study the impact surveillance from different window levels has on street safety. Assuming that each building story is approximately 3 m high, the value of $a_{\max}$ for first-floor windows is 3 m, for first and second-floor windows it is 6 m, and for first, second, and third-floor windows it is 9 m. Second, existing literature indicates that the most reliable distance to observe and interpret an event is 15 m (Amiri and Crain 2020; Jong et al. 2005; Lindsay et al. 2008). Furthermore, events witnessed from a 43-m distance produce weak but reliable eyewitness accounts. Therefore, we divided sightlines into two types: those with $d_{\max} \leq 15$ m and those with $d_{\max} \leq 43$ m. Finally, we defined an angle θ_{fov} as the field of view visible through a window. Outside of this field of view, sightlines were excluded.

Detection and geolocalization of windows. The first step in the calculation of sightlines is the detection of windows on building facades along streets. We collected street-level imagery along the streets of interest and detected windows using the facade labeling algorithm developed by Li et al. (2020). The algorithm detects a set of four key-points (i.e., top-left, bottom-left, bottom-right, and top-right) using 2D heatmaps. Then, it links them together using a neural network trained on labeled images with varying facade structures, viewing angles, lighting, and occlusion conditions. Following this, we calculated the geolocation of each detected window by using and adapting the geolocalization algorithm that was originally developed in Qiu et al. (2019) and later modified in Sharifi Noorian et al. (2020). For each of the detected windows, this process calculates the latitude, longitude, and altitude of the four key-points in the street-level images (Fig. 12.1). We then computed the center-point and stored it as the window's geolocation.

Street and occupant surveillance. To calculate *street surveillance*, we counted all sightlines that have as a starting point the windows with an altitude lower than a_{max} and as an endpoint the location of the street-car camera, with a length lower than $d_{\max}$. The number of these sightlines reflects the number of windows that have unobstructed views to points sampled across the street network (i.e., every 10 m). Regarding *occupant surveillance*, we calculated for each window the number of

Fig. 12.1 Indicative outputs of the facade labeling algorithm developed by Li et al. (2020) on street-level images collected in Amsterdam

neighboring windows that have an unobstructed view (i.e., sightline) to it. Specifically, for each detected window $o_{\text{viewpoint}}$ with an altitude lower than $a_{\max}$, we selected all neighboring windows that had an altitude lower than $a_{\max}$ and were at a maximum distance $d_{\max}$ from each $o_{\text{viewpoint}}$. Next, we calculated all sightlines from the neighboring windows to the $o_{\text{viewpoint}}$ and removed the ones that were obstructed by the presence of intermediate buildings. In particular, for each sightline s, we calculated the angle θ_s between s and the building segment that contains $o_{\text{viewpoint}}$. If $\theta_s > \frac{1}{2}\theta_{fov}$, we considered s outside the field of view of the neighboring window and removed it from the set of sightlines to be considered. Due to the restriction of the sightline angle, a sightline originating from each window ($o_{\text{viewpoint}}$) to each neighboring window (o_{neighbor}) does not imply that the reverse also exists. By repeating these steps for each detected window, we calculated how many neighboring windows have unobstructed views of each window at hand.

To calculate the overall *natural surveillance* scores, we linked all points with a street and occupant surveillance score to a given street segment q. We defined a street segment as a section of the street between two junctions, or between a junction and the end of the street, if the street has a dead end. More specifically, each window was linked to the image where it was detected, and this is, in turn, linked to the corresponding street segment. We calculated the following two scores, normalized by the street segment's length:

$$S_q = \frac{1}{qL} \sum_{i \in P_q} s_i \tag{12.1}$$

$$O_q = \frac{1}{qL} \sum_{i \in P_q} o_i \tag{12.2}$$

where S_q and O_q respectively denote the street and occupant surveillance scores, P_q denotes the set of points linked to a street segment q, q_L is the length of street segment q in meters, and s_i and o_i denote the number of sightlines observing point i.

We further aggregated our scores at the neighborhood level by calculating the sum of the sightlines of all points within each neighborhood, and dividing it by the length of each street segment using the following formulas:

$$S_n = \frac{\sum_{i \in P_n} s_i}{\sum_{i \in Q_n} qL_i} \tag{12.3}$$

$$P_n = \frac{\sum_{i \in P_n} o_i}{\sum_{i \in Q_n} qL_i} \tag{12.4}$$

where S_n and O_n respectively denote the sum of street and occupant surveillance scores within a neighborhood n, Q_n is the set of sampled street segments within n, and P_n is the set of sampled points linked to the street segments within n. As previously stated, we further grouped our scores according to whether the distance between the windows and the corresponding street segment was reliable for witnessing an event ($d_{max} = 15\ m$) or dependable ($d_{max} = 43\ m$).

Correlation analysis. To investigate the relationship between natural surveillance and safety (both actual and perceived), we correlated the street surveillance and occupant surveillance scores with the Amsterdam Safety Index (Gemeente Amsterdam 2015). We first tested the normality of the estimated natural surveillance scores using the Kolmogorov–Smirnov test, which indicated a non-normal distribution. Therefore, for each of the considered neighborhoods, we used Spearman's rank correlation coefficient (*rho*) to calculate the correlation between the natural surveillance scores and the Index's aggregate values and sub-components (i.e., crime, nuisance, and perceived safety).

12.3 Data

We used the city of Amsterdam in the Netherlands as a case study to illustrate and validate how our method could be used to assess a neighborhood's level of natural surveillance. Amsterdam is the capital and most populated city in the Netherlands, characterized by a variety of neighborhoods with equally varying levels of reported (perceived) safety. The city combines a medieval center bustling with tourists all year round with new developments and strictly residential areas in the outskirts. A well-substantiated dataset on (perceived) safety for the entire city of Amsterdam is publicly available, making it an exemplary case to compare our measurements with real-world data on actual and perceived safety. The Amsterdam Safety Index (Gemeente Amsterdam 2015) covers 104 neighborhoods in the city and is composed of three sub-components. These are, namely, the levels of *crime*, *nuisance*, and *perceived safety* in each neighborhood. The lower the index value, the safer the neighborhood is considered to be. We used OpenStreetMap (OSM), an open-source mapping platform, to collect data about the street network and the building footprints. We made use of the *OSMnx* (Boeing 2017) Python library to extract street network data, and the OSM *Overpass* Application Programming Interface (API) to collect the building footprints. Moreover, we used the Google Street View Static API to detect the location of windows on the building facades along the street segments. Due to budget limitations, we focused on 40 out of the 104 Amsterdam neighborhoods covered by the Safety Index. Neighborhoods were selected such that they are spatially contiguous (i.e., they share a common administrative boundary) and are characterized by a variety of safety index scores. In the final subset of 40 neighborhoods (Fig. 12.2), we collected 6,667 street segments from OSM and 109,988 street-level images from Google Street View along the street segments, with the maximum allowed resolution of 640 $\times$ 640 pixels and with orthogonal field of view and zero pitch to capture the building facades. The window detection and geo-localization algorithms provided a total of 872,360 windows, extracted with the use of the ResNet18 model for facade labeling.

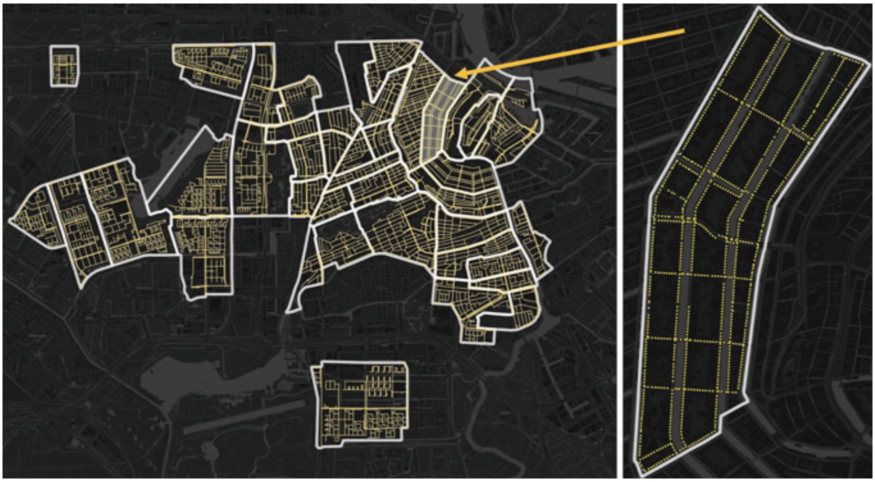

Fig. 12.2 Left: The 40 neighborhoods and their streets considered in our analysis. Right: An example of the geolocations of street-level images collected along street segments in Amsterdam's Grachtengordel-West neighborhood

12.4 Results

This section provides an overview of the application of our method for estimating natural surveillance in Amsterdam, the Netherlands. We also present the correlation results between our measurements of street and occupant surveillance and the 2019 Amsterdam Safety Index and its sub-components, namely crime, nuisance, and perceived safety in each of the considered neighborhoods. Furthermore, we compared the influence of considering windows from different floor levels and distances from the street on indicating a neighborhood's actual and perceived safety levels.

Figure 12.3 illustrates the calculated street and occupant surveillance scores, considering windows within a distance of 43 m from the streets and up to the first floor of the buildings, together with the overall Safety Index values of the 40 considered neighborhoods. We converted each of these scores into three categorical variables, namely, low, medium, and high, according to the tertile they belong to. This allows for easier visual comparison, given that each of the presented metrics is originally expressed in different units.

Most neighborhoods showcased consistency across the three scores, routinely resulting in high or low safety areas. Indicative examples of this include the Burgwallen- Oude Zijde (BOZ) and Burgwallen-Nieuwe Zijde (BNZ) neighborhoods, both in the historical center of Amsterdam, consistently scoring low across all metrics. Similarly, neighborhoods such as Museumkwartier (MU) and Staatsliedenbuurt (ST) consistently scored among the safest. Examples of the opposite include Buitenveldert-West (BW), which scored low in terms of street surveillance, medium in occupant surveillance, and high in the Safety Index values. Figure 12.3 further

Fig. 12.3 **a** Street surveillance scores; **b** Occupant surveillance scores; **c** Amsterdam Safety Index values for the 40 considered Amsterdam neighborhoods, classified into tertiles

zooms in on the street structure of select neighborhoods to elucidate the individual contributions of street segments to the overall street and occupant surveillance scores.

Table 12.1 shows the results of the correlation between our street and occupant surveillance scores and the Amsterdam Safety Index and its sub-components, using the Spearman's rank correlation coefficient (*rho*). The results yielded a moderate negative and statistically significant correlation ($r = -0.49$, $p < 0.001$) between street surveillance and Safety Index values in the case of sightlines with $d_{max} = 43$ m and up to the first floor of buildings (i.e., 1F). The correlation became weaker when we considered sightlines from buildings within a 15 m distance, or from higher floors. Looking at the Index's sub-components, the correlation between street surveillance and *crime* or *nuisance* also became weaker when we considered sightlines originating from floors higher than the first. Also, street surveillance scores generally presented strong negative correlations with *perceived safety* values, with sightlines of 15-m length yielding the strongest results. The correlations of occupant surveillance scores with the Safety Index and its sub-components were generally weaker in comparison with their street surveillance counterparts. The occupant surveillance scores had the highest correlation with the average Safety Index values ($r = 0.34$).

The use of a locally weighted scatter plot smoothing (LOWESS) regression to examine the linearity of the relationship between the different scores, as shown in Fig. 12.4, provided additional insight into the correlations. Specifically, the comparison of the street surveillance scores with the overall Safety Index (Panel I) and the perceived safety sub-component (Panel II) yielded an interesting non-linear pattern.

Table 12.1 Spearman correlations of the street and occupant surveillance scores with the 2019 Amsterdam Safety Index

Correlations of street and occupant surveillance with the Amsterdam Safety Index							
Index and sub-components	Maximum sightline length						
	15 m (reliable)			43 m (dependable)			None
	Included floors						
	1F	≤2F	≤3F	1F	≤ 2F	≤ 3F	All
	Street surveillance						
Safety Index	−0.45 **	−0.38*	−0.39*	**−0.49****	−0.42**	−0.40*	−0.45**
Crime	−0.34*	−0.30	−0.31	**−0.40***	−0.37*	−0.34*	−0.33*
Nuisance	−0.23	−0.18	−0.15	**−0.29**	−0.21	−0.18	−0.27
Perceived Safety	**−0.48****	−0.43**	−0.44**	−0.45**	−0.36*	−0.38*	−0.43**
	Occupant surveillance						
Safety Index	−0.34*	−0.38*	−0.39*	−0.40*	**−0.41***	−0.38*	
Crime	−0.23	−0.33*	−0.34*	−0.31*	**−0.35***	−0.31	
Nuisance	−0.25	−0.22	−0.20	**−0.32***	−0.24	−0.19	
Perceived Safety	**−0.36***	−0.35*	**−0.36***	−0.32**	−0.33*	−0.35*	

$* = p <= 0.05$, $** = p <= 0.01$

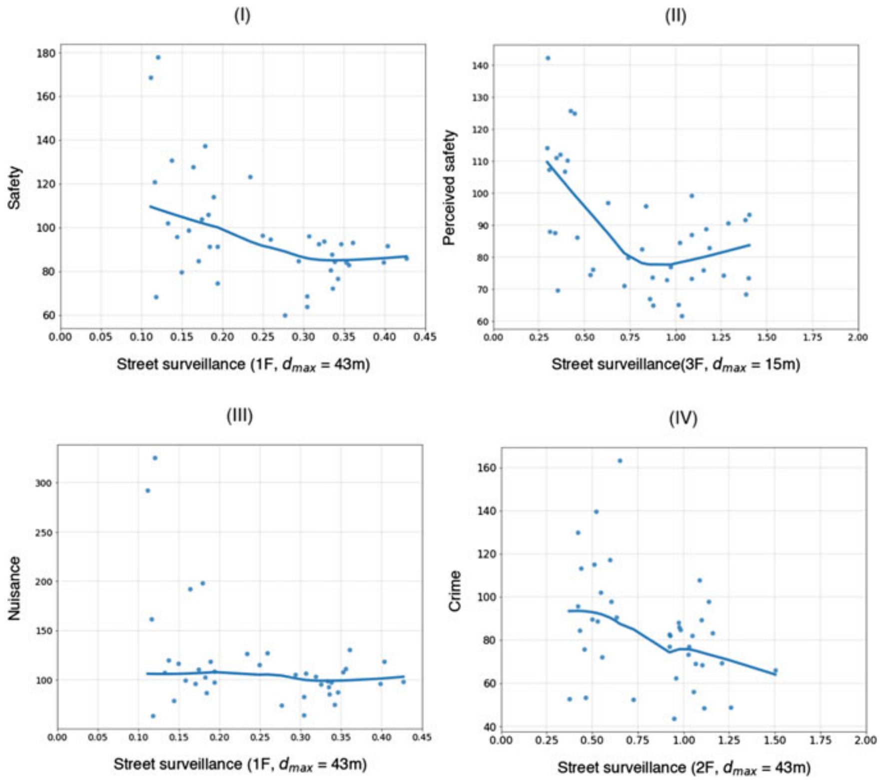

Fig. 12.4 Scatter plots and corresponding trendlines depicting the relationship between estimated street surveillance scores and the Amsterdam Safety Index (I) and its sub-components: perceived safety (II); nuisance (III); crime (IV)

We observed that as the street surveillance score increased, the trendline became relatively horizontal from a certain point onward. This suggests that even though an increased level of street surveillance is generally associated with higher safety—either actual or perceived—this association becomes weaker after a certain value (approximately 0.3 for safety and 0.8 for perceived safety). However, this does not seem to be the case when it comes to the association of street surveillance with the levels of nuisance (Panel III) and crime (Panel IV). The corresponding scatter plots and trendlines did not indicate any particular pattern.

12.5 Discussion

The application of our method in several neighborhoods in Amsterdam demonstrated that the combination of street-level imagery with computer vision techniques offers a promising approach to measuring natural surveillance across large spatial extents. As such, it can provide a pathway to integrate the widely advocated, yet difficult to capture, notion of "eyes on the street" into the planning and design for safer neighborhoods. We also showed that different aspects of surveillance (i.e., street or occupant-based) have varying contributions to a neighborhood's overall level of safety and elicit interesting non-linear relationships.

Our results suggest an overall significant negative correlation between our average natural surveillance scores and the Safety Index. Given that lower Index values indicated safer neighborhoods, an increased level of natural surveillance correspondingly indicated a safer neighborhood. This aligns with related expectations from the CPTED literature (Cozens and Love 2015; Crowe 2000). We specifically detected stronger correlations between street surveillance scores and the Safety Index, whereas the correlations with occupant surveillance scores appeared weaker. This suggests that the degree of street visibility from surrounding windows is a stronger predictor of a street's level of natural surveillance compared to window visibility from surrounding buildings.

Our analysis also uncovers aspects of natural surveillance that have largely been overlooked in the existing evidence base. Our findings, in particular, support our hypothesis that window levels and the distance of buildings from the street influence how natural surveillance correlates with overall safety. However, variations do exist between the two different facets of natural surveillance. Specifically, street visibility (i.e., street surveillance) from first-floor windows correlates most with the average values of the Safety Index and this association becomes stronger as the distance from the street increases. This appears to be less the case when it comes to the visibility of windows from surrounding buildings (i.e., occupant surveillance). We also observed a strong correlation between street surveillance and perceived safety. The consideration of different floor levels barely influenced this correlation. However, the distance of the windows from the street did influence this association, with windows closer to the street (i.e., sightlines with a length of 15 m) leading to stronger correlations.

The overall strong association between street surveillance and perceived safety would generally suggest that the higher the level of street surveillance, the more it would correlate with an increased perception of safety. However, our analysis of linearity indicates a natural surveillance threshold value above which the level of perceived safety remains relatively stable. Figure 12.4 (Panel I) shows that street segments with street surveillance score up to 0.3—this corresponds to an average of three windows overlooking a 10-m-long street segment—accordingly led to a gradually increasing level of neighborhood safety. However, street surveillance scores of 0.3 and above did not lead to any increases in the overall level of safety. Figure 12.5 provides indicative examples of streets with street surveillance scores of 0, 0.15, 0.3, and 0.7 to showcase what streets of low or high street surveillance are like. This

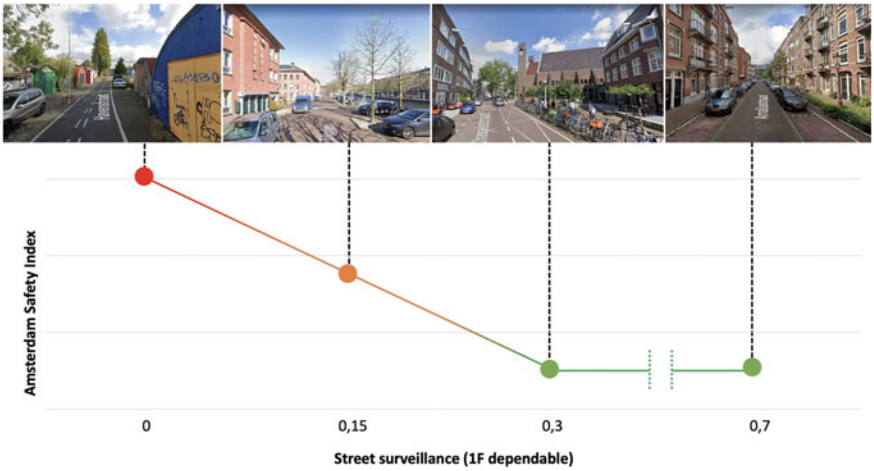

Fig. 12.5 A selection of Amsterdam streets, along with their street surveillance scores (1F reliable). Streets included in the figure, from left to right: Havenstraat, De Rijpgracht, Chasse' straat and Amaliastraat. As the street surveillance score rises to 0.3, neighborhoods feel safer. An increase to 0.7 does not appear to be associated with increased (perceived) safety

result provides an interesting insight into *how much* and *what kinds* of street features lead to increased (feelings of) safety and requires further research in different urban environments.

There are several limitations in this study that could be addressed in future research. First, our method depends on how well windows are depicted in street-level imagery. Some windows, however, are excluded from the street-level images either due to a lack of imagery along certain street segments or because the view from the street to the window is obstructed (e.g., by a tree). Second, the facade labeling algorithm used for window detection is occasionally inaccurate. Indicative inaccuracies include windows that are in shadow or with occluded openings, as well as storefront windows that may go undetected by the algorithm because it was trained on images of residential buildings (Li et al. 2020). Nonetheless, the facade labeling algorithm we used was tested on several datasets of building facade images and achieved a pixel accuracy of 90% on average (Korc and Förstner 2009; Riemenschneider et al. 2012; Teboul et al. 2011). Third, the geolocalization algorithm can introduce errors (namely, mean error of 1.07 m and standard deviation of 1.09 m), the most significant of which are caused by inaccurate GPS metadata in street-level images. Fourth, natural surveillance is a broad concept that encompasses more than window-based surveillance. In fact, active street observation is largely dependent on residents' time, willingness, and capacity to watch and defend their streets and communities (Cozens 2015). Therefore, our research could be expanded to take into account other factors that influence natural surveillance, such as citizens' daily activity patterns, time of day, or street lighting quality. Lastly, we only tested and evaluated our method in a few Amsterdam neighborhoods. For this reason, we intend to broaden the applicability of our method by implementing it in other cities.

12.6 Conclusion

Natural surveillance has drawn a lot of interest and is now a crucial component of design strategies aimed at improving actual and perceived safety in urban spaces. This paper introduced a method for measuring natural surveillance at scale by leveraging a combination of street-level imagery and computer vision techniques. Our work has practical value for built-environment professionals who seek to understand and improve the levels of actual and perceived safety in urban neighborhoods. Specifically, our method draws on the new possibilities offered by street-level imagery in capturing built-environment features, such as the location of windows and any visibility blockages that have been shown to affect natural surveillance. It also employs geolocalization and facade labeling techniques to estimate the surveillance of windows from the street level and surrounding buildings across large spatial extents. We applied our method in neighborhoods of Amsterdam and correlated our measurements with various components comprising the city's Safety Index to validate its use as an estimator of neighborhood safety. Our analysis showcased that our method can be a promising and scalable alternative to the manual collection of observations around aspects of natural surveillance. Our results align with existing evidence from the CPTED literature and suggest that surveillance of windows from the street contributes more to the overall safety than surrounding buildings. Moreover, the window level and distance of buildings from the street appear to have varying influences on the feeling of safety. Another intriguing finding from our analysis is the identification of a natural surveillance threshold point, with scores above it not resulting in increased (perceived) safety. However, more research in different urban settings is required to provide more evidence of this. In particular, it presents an interesting avenue of future research in the fields of environmental criminology and next-generation CPTED (Saville and Cleveland 2008) that can contribute to an improved understanding of what kinds of built-environment characteristics lead to increased (feelings of) safety.

Acknowledgements Vasileios Milias, Alessandro Bozzon, and Achilleas Psyllidis acknowledge support from the European Union's Horizon 2020 research and innovation program under grant agreement No. 874724.

Author Contribution Statement Timo Van Asten and Vasileios Milias equally contributed to the study conception, research design, methodology, data analysis, and writing of the draft and revised manuscripts. Alessandro Bozzon contributed to the research design, funding acquisition, resources, supervision, review, and editing of the manuscript. Achilleas Psyllidis contributed to the study conception, research design, methodology, funding acquisition, resources, supervision, and writing of the draft and revised manuscripts.

References

Amiri S, Crain DR (2020) Quantifying jacobs' notion of 'eyes upon the street' in 3-dimensions. J Urban Des 25(4):467–485. https://doi.org/10.1080/13574809.2019.1691440,URL

Barnett DW, Barnett A, Nathan A, Van Cauwenberg J, Cerin E (2017) Built environmental correlates of older adults' total physical activity and walking: a systematic review and meta-analysis. Int J Behav Nutr Phys Act 14(1):1–24

Barton H (2010) Strengthening the roots of planning. Plan Theory Pract 11(1):95–101

Boeing G (2017) Osmnx: New methods for acquiring, constructing, analyzing, and visualizing complex street networks. Comput Environ Urban Syst 65:126–139. https://doi.org/10.1016/j.compenvurbsys.2017.05.004, http://arxiv.org/pdf/1611.01890

Carmona M (2021) Public places urban spaces: the dimensions of urban design. Routledge

Cozens P, Hillier D (2012) Revisiting Jane Jacobs's 'eyes on the street' for the twenty- first century: evidence from environmental criminology, Routledge, pp 196–214. https://doi.org/10.4324/9780203095171

Cozens P, Love T (2015) A review and current status of crime prevention through environmental design (cpted). J Plan Lit 30(4):393–412

Cozens P (2015) Crime and community safety: challenging the design consensus. In: The Routledge handbook of planning for health and well-being, Routledge, pp 196–211

Crowe TD (2000) Crime prevention through environmental design: applications of architectural design and space management concepts, 2nd edn. Butterworth- Heinemann, Boston, Mass

Foster S, Giles-Corti B (2008) The built environment, neighborhood crime and constrained physical activity: an exploration of inconsistent findings. Prev Med 47(3):241–251

Foster S, Giles-Corti B, Knuiman M (2011) Creating safe walkable streetscapes: does house design and upkeep discourage incivilities in suburban neigh-bourhoods? J Environ Psychol 31(1):79–88. https://doi.org/10.1016/j.jenvp.2010.03.005

Gemeente Amsterdam (2015) Verantwoordingsdocument veiligheidsindex 2014. Report

Groshong L, Wilhelm Stanis SA, Kaczynski AT, Hipp JA (2020) Attitudes about perceived park safety among residents in low-income and high minority kansas city, missouri, neighborhoods. Environ Behav 52(6):639–665

Jackson J, Stafford M (2009) Public health and fear of crime: a prospective cohort study. Br J Criminol 49(6):832–847

Jacobs J (1961) The death and life of great American cities

Jong MD, Wagenaar WA, Wolters G, Verstijnen IM (2005) Familiar face recognition as a function of distance and illumination: a practical tool for use in the courtroom. Psychol Crime Law 11(1):87–97. https://doi.org/10.1080/10683160410001715123

Korc F, Förstner W (2009) eTRIMS image database for interpreting images of man-made scenes. Dept of Photogrammetry, University of Bonn, Tech Rep TR-IGG-P-2009-01

Lee I, Jung S, Lee J, Macdonald E (2017) Street crime prediction model based on the physical characteristics of a streetscape: analysis of streets in low-rise housing areas in south korea. Environ Plann B Urban Analytics City Sci 46(5):862–879. https://doi.org/10.1177/2399808317735105

Li CK, Zhang HX, Liu JX, Zhang YQ, Zou SC, Fang YT (2020) Window detection in facades using heatmap fusion. J Comput Sci Technol 35(4):900–912. https://doi.org/10.1007/s11390-020-0253-4, http://jcst.ict.ac.cn/CN/abstract/article2660.shtml

Lindsay RC, Semmler C, Weber N, Brewer N, Lindsay MR (2008) How variations in distance affect eyewitness reports and identification accuracy. Law Hum Behav 32(6):526–535. https://doi.org/10.1007/s10979-008-9128-x

Mason P, Kearns A, Livingston M (2013) "safe going": the influence of crime rates and perceived crime and safety on walking in deprived neighbourhoods. Soc Sci Med 91:15–24

De Nadai M, Xu Y, Letouze´ E, Gonza´lez MC, Lepri B (2020) Socio-economic, built environment, and mobility conditions associated with crime: a study of multiple cities. Sci Rep 10(1). https://doi.org/10.1038/s41598-020-70808-2

Newman O (1972) Defensible space. Macmillan New York

Peeters M, Vander Beken T (2017) The relation of cpted characteristics to the risk of residential burglary in and outside the city center of ghent. Appl Geogr 86:283–291. https://doi.org/10.1016/j.apgeog.2017.06.012

Qiu S, Psyllidis A, Bozzon A, Houben GJ (2019) Crowd-mapping urban objects from street-level imagery. In: The world wide web conference on-WWW '19, ACM Press. https://doi.org/10.1145/3308558.3313651

Reynald DM, Elffers H (2009) The future of newman's defensible space theory. European J Criminol 6(1):25–46. https://doi.org/10.1177/1477370808098103

Riemen-schneider H, Krispel U, Thaller W, Donoser M, Havemann S, Fellner D, Bischof H (2012) Irregular lattices for complex shape grammar facade parsing. In: 2012 IEEE conference on computer vision and pattern recognition, IEEE, pp 1640–1647

Rydin Y, Bleahu A, Davies M, Dávila JD, Friel S, De Grandis G, Groce N, Hallal PC, Hamilton I, Howden-Chapman P et al (2012) Shaping cities for health: complexity and the planning of urban environments in the 21st century. The Lancet 379(9831):2079–2108

Saville G, Cleveland G (2008) Second-generation cpted: The rise and fall of oppor- tunity theory. In: 21st century security and CPTED, Auerbach Publications, pp 93–104

Shach-Pinsly D (2019) Measuring security in the built environment: evaluating urban vulnerability in a human-scale urban form. Landsc Urban Plan 191:103412. https://doi.org/10.1016/j.landurbplan.2018.08.022

Sharifi Noorian S, Qiu S, Psyllidis A, Bozzon A, Houben GJ (2020) Detecting, classifying, and mapping retail storefronts using street-level imagery. In: Proceedings of the 2020 international conference on multimedia retrieval, ACM. https://doi.org/10.1145/3372278.3390706

Stafford M, Chandola T, Marmot M (2007) Association between fear of crime and mental health and physical functioning. Am J Public Health 97(11):2076–2081

Teboul O, Kokkinos I, Simon L, Koutsourakis P, Paragios N (2011) Shape grammar parsing via reinforcement learning. In: CVPR 2011, IEEE, pp 2273–2280

UN-Habitat (2020) United nations system-wide guidelines on safer cities and human settlements. Report

Won J, Lee C, Forjuoh SN, Ory MG (2016) Neighborhood safety factors associated with older adults' health-related outcomes: a systematic literature review. Soc Sci Med 165:177–186